Pulse decomposition analysis in camera-based photoplethysmography

Michele Sorelli, Carlotta Kopietz, Sebastian Zaunseder, Leonardo Bocchi

Angaben zur Veröffentlichung / Publication details:

Sorelli, Michele, Carlotta Kopietz, Sebastian Zaunseder, and Leonardo Bocchi. 2019. "Pulse decomposition analysis in camera-based photoplethysmography." In *41st Annual International Conference of the IEEE Engineering in Medicine and Biology Society (EMBC), 23-27 July 2019, Berlin, Germany*, edited by Thomas Prenzel, Thomas Lenarz, Mohamad Sawan, and Riccardo Barbieri, 3179–82. Piscataway, NJ: IEEE. https://doi.org/10.1109/embc.2019.8857856.

Pulse decomposition analysis in camera-based photoplethysmography

Michele Sorelli[1], Carlotta Kopietz[2], Sebastian Zaunseder[3] and Leonardo Bocchi[1]

Abstract— **Imaging photoplethysmography (iPPG) is an interesting alternative to laser speckle contrast imaging for the analysis of spatio-temporal patterns in the cutaneous microcirculation. Recent years have witnessed the development of sophisticated techniques for the non-invasive extraction of vascular-related features. These techniques, referred to as *pulse decomposition algorithms* (PDA), most often involve the analysis of photoplethysmographic waves. This study validated the use of a multi-Gaussian (PDA) for the automatic mapping of iPPG pulse waveforms acquired with a standard camera. We show that iPPG-based PDA can reveal differences in skin perfusion in response to cold stimuli. The study thus proves the potential for morphological analyses of the iPPG pulse waveform.**

I. Introduction

Camera-based photoplethysmography, commonly referred to as *imaging photoplethysmography* (iPPG), is a low-cost technique which enables the contactless spatio-temporal analysis of the cutaneous perfusion [1]. This modality is based on the time-varying modulation of the light reflected at the skin interface due to the blood pulsatility produced by the activity of the cardiac pump [2], [3], [4]. The vast majority of works in the field of iPPG mainly focuses on heart rate extraction [1]. However, in recent years, more sophisticated techniques able to provide a non-invasive assessment of arterial stiffness [5] and distal pulse reflection [6] have been developed for conventional PPG. The general concept underlying these methods is that the fluid mechanics of the vascular system exerts an observable effect on the characteristic shape of peripheral pulse waveforms [7]. In this regard, *pulse decomposition algorithms* (PDAs) have recently emerged as a valuable method for their accurate reconstruction and analysis [8], [9], [10], [11]. In general, PDAs are able to model PPG or laser Doppler flowmetry pulse waves as a linear combination of a varying number of basic components (e.g. normal, log-normal, gamma or Rayleigh functions), where each secondary term is theoretically meant to reproduce a reflection wave originating from vascular impedance inhomogeneities.

The objective of the present study was to assess the ability of a novel multi-Gaussian PDA [12] to accurately reconstruct iPPG waveforms and yield parameters to characterize the cutaneous perfusion. To this end, the vasoconstrictive effect induced by a localized cold stimulation was adopted as a test case, in order to evaluate the sensitivity of the algorithm to the expected attenuation of the cutaneous blood perfusion.

[1] Department of Information Engineering, University of Florence, Italy leonardo.bocchi@unifi.it

[2] Institute of Biomedical Engineering, Technical University of Dresden, Germany

[3] Faculty of Information Technology, Dortmund University of Applied Sciences and Arts, Germany

II. Materials and methods

A. Subjects and measurement protocol

This work relied on a set of videos recorded during a recent experimental study by Zaunseder et al. [13]. The study aimed at assessing the capability of standard RGB cameras to detect changes in the cutaneous microvascular perfusion, in response to the application of a non-invasive cold (i.e. vasoconstrictive) stimulus.

Specifically, the present analysis used videos captured from 15 healthy subjects (age: 26 ± 6 years; M/F: 11/4) by means of a high-speed UI-3370CP-C-HQ camera (IDS Imaging Development Systems, Germany). The original study had been approved by the Institutional Review Board of the Technical University of Dresden (ID: EK168052013): all the participants provided their informed consent prior to the measurement sessions. The acquisitions were performed under fluorescent ceiling illumination, with the subjects lying supine. In detail, videos were captured at 100 fps, with a 420x320 pixel image resolution and a color depth of 12 bit, at an approximate distance of 80 cm, so as to include the face and part of the upper torso in the camera field of view. The cold stimulus consisted in the application of an ice pack ($T < 0\,^{\circ}C$) on the subjects' forehead for 30 s. The original experimental protocol included three successive phases of cold stimulation, separated by time intervals where the basal perfusion levels were restored; the final dataset was thus comprised of 45 matched *pre-cooling*/*post-cooling* time series of 10 s (i.e. 3 per subject), defined immediately before and after each cold stimulus. Due to the time gap separating the repeated stimuli, each pair was assumed to be statistically independent in the following statistical analysis.

B. iPPG signal generation

The iPPG signals were generated from a region of interest (ROI) centered on the subjects' forehead, so as not to include any disturbing elements (e.g. hair). The multi-Gaussian PDA was applied only to the green channel of the captured videos, as it carries the highest sensitivity to the blood pulsatility.

The captured videos were first inverted, since the intensity of the backscattered green light is inversely related to the local blood concentration. Then, a spatial 15x15 pixel moving average filter was applied to improve the image SNR, followed by a temporal 5-order IIR Butterworth low-pass filter with cut-off frequency 3.3 Hz, introduced for suppressing the *unphysiological* noisy components beyond the heart rate range. The iPPG signal was finally obtained by averaging the gray level intensities inside the entire ROI.

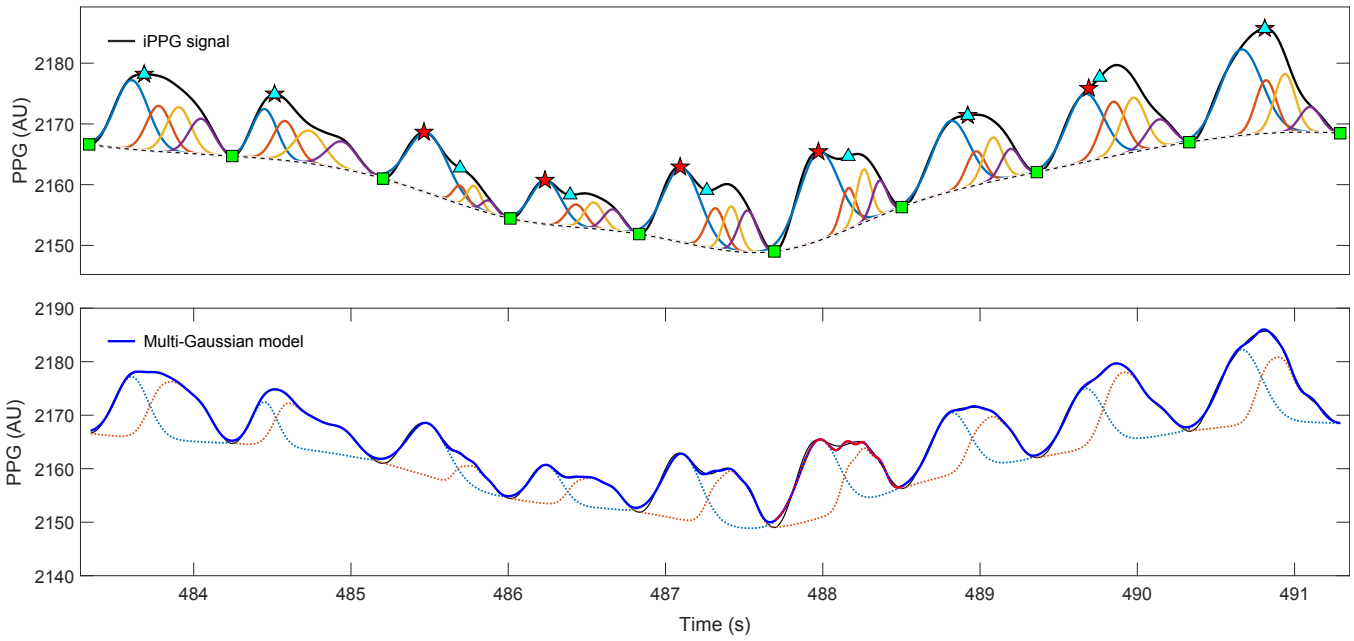

Fig. 1. Multi-Gaussian decomposition of the iPPG pulse wave: single components (top) and general model (bottom). *Red* stars mark the systolic references, whereas *light blue* triangles correspond to the incisura dividing the systolic and diastolic phases of each cardiac cycle (identified by the *green* squares). In this example, the sixth pulse (highlighted in red) had been identified as a probable misfitted instance, and accordingly excluded from further analysis.

C. PDA for camera-based PPG

The extracted iPPG data were processed with a modified version of a multi-Gaussian PDA recently developed for the analysis of laser Doppler flowmetry pulse waveforms. As thoroughly described in [12], the first *detection* stage of the algorithm performs the automatic windowing of the cardiac cycles and the identification of systolic and dicrotic markers which are needed during the subsequent modeling of the iPPG pulse contour (Fig. 1 *top*).

In detail, the PDA first identifies the local maxima of the iPPG signal as *systolic* reference points (Fig. 1 *top*, red stars), imposing an upper threshold of 150 bpm on the resultant instantaneous heart rate, in order to restrict the amount of *false positive* detections. Next, it searches for any local minima between consecutive systolic peaks to obtain a preliminary detection of the cardiac cycles to be analyzed (Fig. 1 *top*, green squares): at this stage, if more than one minimum is found, the algorithm selects the closest detection to the systolic peak, whose amplitude difference with respect to the absolute minimum is below 15% of Δp, i.e. the amplitude range between the systolic peak and the lowest detected minimum; otherwise, the latter is kept as end-diastolic marker.

Afterwards, the algorithm examines the accuracy of the above detections: if the time delay between two consecutive end-diastolic valleys is lower than 80% of the median duration of the identified cardiac cycles, then the corresponding window is marked as "short"; next, consecutive "short" intervals are detected, and the separating valley is deleted together with the corresponding systolic peak (being likely related to a secondary ripple, splitting the *true* cardiac cycle). Vice versa, if the resulting cardiac cycle is longer then 180% of the median length, a new arbitrary end-diastolic marker is added to its center (so as to divide two cycles which had been spuriously merged); then, the corresponding time windows are marked so as to be excluded from further consideration. This step is fundamental to the accurate detrending of the cardiac pulsatility, as explained in the following. Furthermore, a second refinement mechanism is implemented with the aim of improving the preliminary systolic markers. In specific, the algorithm tries to detect any local minima in the first derivative of the iPPG signal (computed by means of a 3-point differentiator), inside the interval between the original peak and the instant corresponding to 20% of the cardiac cycle duration; if such inflection points are present, the algorithm seeks any maxima inside the above time window, selecting as new reference the earliest peak whose amplitude exceeds 67% of Δp; otherwise, the earliest inflection point above $0.2 \cdot \Delta p$ is selected.

Afterwards, the iPPG signal is detrended through a cubic spline interpolation of the end-diastolic references and the absolute minima between the refined systolic peaks (Fig.1), in order to isolate the cardiac oscillatory component to be modeled. At this stage, the provisional end-diastolic markers are substituted for possible local minima, closer to the systolic peak, if the amplitude change does not exceed $0.2 \cdot \Delta p$.

Finally, a further *dicrotic* inflection point (Fig. 1 *top*, light blue triangles), intended to identify the systolic and diastolic phases of the waveform, is detected to the right of the systolic peak. The technique adopted in this regard is identical to the one reported in [12], except for marginal modifications.

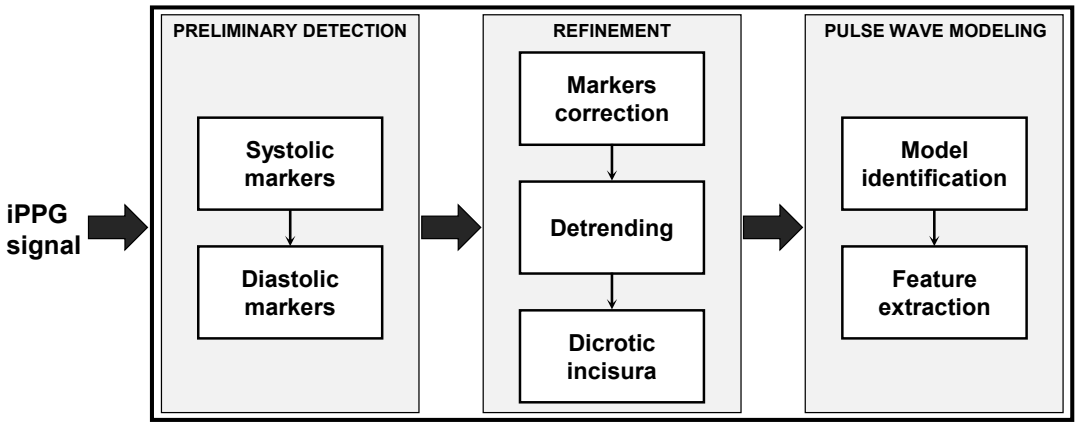

Fig. 2. Multi-Gaussian *pulse decomposition algorithm*: block diagram.

Following the initial detection stage, a four-component Gaussian model is iteratively fitted to each identified pulse, in order to derive a parametric representation of its waveform. The fitting of the iPPG data was performed with a trust region approach for nonlinear optimization problems. The configuration of the optimization algorithm is detailed in [12]: in general, the initial and boundary values assigned to the twelve free parameters of the multi-Gaussian model are adapted to the amplitude and temporal properties of each cardiac cycle, in order to improve the accuracy of the fitting process; namely, the algorithm is designed so that only one of the four Gaussian components is used for reproducing the systolic interval to the left of the *dicrotic* inflection point. At the end of the modeling stage, a series of exclusion criteria is imposed on the identified parameters to detect residual *false* cardiac cycles and, secondly, to exclude misfitted pulse waves from further consideration [12].

Afterwards, the developed PDA performs a detailed characterization of the identified waveform models, through the following quantitative shape features:

$$\vec{f} = \Big(a_1, a_2, a_3, a_4, \Delta t_{1-2}, \Delta t_{1-3}, \Delta t_{1-4}, \mathrm{SI}, \mathrm{RI}, \mathrm{CT}\Big), \quad (1)$$

where a_i is the amplitude of the i^{th} Gaussian, while Δt_{1-2}, Δt_{1-3}, and Δt_{1-4} represent the relative delays of the secondary components with respect to the main systolic pulse. Furthermore, the adopted feature vector includes the following properties: the *crest time* (CT), i.e. the rise time from the start of the cardiac cycle to the identified peak of the systolic Gaussian; a large artery *stiffness index* (SI) [5], estimated by dividing the subject's height by the time delay between the first systolic Gaussian and the centroid of the reconstructed diastolic contour; and, finally, an index of peripheral vascular tone, termed *reflection index* (RI) [6], computed as the ratio of the areas under the diastolic and systolic phases of the pulse model. Average values of these features were used to characterize each processed time interval of the iPPG signals (defined in Section II-A).

D. Statistical analysis

The statistical analysis was carried out with the SPSS software (Version 21.0; IBM corp., US). Data normality was assessed by means of a preliminary Shapiro-Wilk test: since each feature was related to significantly non-normal distributions in either the reference or cooling phases, the non-parametric Wilcoxon signed-rank test for related samples was selected for detecting the presence of significant effects on the iPPG data. However, the available sample size of 45 observations limited the scope of the analysis to moderate-to-large trends (Cohen's $d \approx 0.4$) at a significance level $\alpha = 0.05$ and power $1-\beta = 0.8$, as assessed by means of a post-hoc sensitivity analysis, performed with the G*Power 3 software [14] for statistical power analysis.

III. Results

The quality of the multi-Gaussian model of the iPPG pulse waveforms was inspected through the analysis of the average coefficient of determination R^2, related to each modeled iPPG pulse and, furthermore, through a normalized goodness of fit metric, defined for each iPPG signal as:

$$G_n = 1 - \frac{\|\mathrm{iPPG}(t) - M_g(t)\|}{\|\mathrm{iPPG}(t) - \langle \mathrm{iPPG}(t) \rangle\|}, \quad (2)$$

where $M_g(t)$ represents the multi-Gaussian model, whereas $\langle\cdot\rangle$ indicates time averaging. Over the available dataset of 90 iPPG time series, the algorithm achieved a mean R^2 of 0.993 ± 0.007 ($\pm\sigma$) and a mean G_n equal to 0.941 ± 0.039, demonstrating an extremely high accuracy and reliability in reproducing the iPPG waveforms.

The results of the statistical comparison between the time-averaged features of the iPPG pulse wave, obtained from matched pairs of *pre-cooling* and *post-cooling* intervals, individually associated with a pulse detection rate $> 60\%$ (following the application of the exclusion criteria), are summarized in Table I. A statistically significant increase of the CT and the relative delays Δt_{1-i} of the *diastolic* Gaussians was detected, together with a consistent decrease of the arterial SI. A significant decrease of the a_1, a_2 and a_3 amplitudes was also observed; this expected effect, however, was not mirrored by a significant alteration of the distal RI.

TABLE I

COMPARISON OF THE IPPG WAVEFORM FEATURES, BEFORE AND AFTER THE APPLICATION OF THE COLD STIMULUS.

FEATURE		BASELINE		COOLING		p value
		$\langle\cdot\rangle$	σ	$\langle\cdot\rangle$	σ	
a_1	[AU]	10.7	4.5	9.4	3.7	0.005†
a_2	[AU]	6.0	2.5	5.3	2.1	0.005†
a_3	[AU]	6.4	2.5	5.7	2.2	0.01†
a_4	[AU]	4.5	1.7	4.1	1.5	0.122
SI	[m/s]	7.0	1.5	6.4	1.1	<0.001†
RI	[%]	104.1	24.4	111.3	33.3	0.509
CT	[ms]	264	38	276	33	0.05†
Δt_{1-2}	[ms]	168	40	182	34	0.006†
Δt_{1-3}	[ms]	279	60	298	54	<0.001†
Δt_{1-4}	[ms]	402	96	432	87	<0.001†

†: statistically significant;
$\langle\cdot\rangle$: time average.

IV. CONCLUSIONS

Collectively, the findings of the present preliminary study support the suitability of PDAs for the automatic detection and analysis of iPPG pulse waveforms. This is strongly demonstrated by the goodness of fit exhibited by the four-component Gaussian model. Furthermore, a mild modification of the adopted amplitude and temporal features of the iPPG pulse model (Eq.1) was detected in response to a local cold stimulation.

Thus, the proposed technique appears to be sensitive to the vasoconstrictive effect of this non-invasive stimulus and might enable the contactless evaluation of the neurovascular pathways underlying this physiological vasomotor response.

REFERENCES

[1] S. Zaunseder, A. Trumpp, D. Wedekind, and H. Malberg, "Cardiovascular assessment by imaging photoplethysmography–a review," *Biomedical Engineering/Biomedizinische Technik*, vol. 63, no. 5, pp. 617–634, 2018.

[2] J. Allen, "Photoplethysmography and its application in clinical physiological measurement," *Physiological Measurement*, vol. 28, no. 3, p. R1, 2007.

[3] A. A. Kamshilin, V. Teplov, E. Nippolainen, S. Miridonov, and R. Giniatullin, "Variability of microcirculation detected by blood pulsation imaging," *PLoS ONE*, vol. 8, no. 2, pp. 1–9, 2013.

[4] L. Frassineti, F. Giardini, A. Perrella, M. Sorelli, L. Sacconi, and L. Bocchi, "Evaluation of spatial distribution of skin blood flow using optical imaging," in *CMBEBIH 2017*. Springer, 2017, pp. 74–80.

[5] S. C. Millasseau, R. Kelly, J. M. Ritter, and P. J. Chowienczyk, "Determination of age-related increases in large artery stiffness by digital pulse contour analysis," *Clinical Science*, vol. 103, no. 4, pp. 371–377, 2002.

[6] ——, "The vascular impact of aging and vasoactive drugs: comparison of two digital volume pulse measurements," *American Journal of Hypertension*, vol. 16, pp. 467–472, 2003.

[7] J. Alastruey, T. Passerini, L. Formaggia, and J. Peiró, "Physical determining factors of the arterial pulse waveform: theoretical analysis and calculation using the 1-D formulation," *Journal of Engineering Mathematics*, vol. 77, no. 1, pp. 19–37, 2012.

[8] M. C. Baruch, D. E. R. Warburton, S. S. D. Bredin, A. Cote, D. W. Gerdt, and C. M. Adkins, "Pulse Decomposition Analysis of the digital arterial pulse during hemorrhage simulation," *Nonlinear Biomedical Physics*, vol. 5, no. 1, 2011.

[9] L. Wang, L. Xu, S. Feng, M. Q.-H. Meng, and K. Wang, "Multi-gaussian fitting for pulse waveform using weighted least squares and multi-criteria decision making method," *Computers in Biology and Medicine*, vol. 43, no. 11, pp. 1661–1672, 2013.

[10] R. Couceiro, P. Carvalho, R. Paiva, J. Henriques, I. Quintal, M. Antunes, J. Muehlsteff, C. Eickholt, C. Brinkmeyer, M. Kelm, *et al.*, "Assessment of cardiovascular function from multi-gaussian fitting of a finger photoplethysmogram," *Physiological Measurement*, vol. 36, no. 9, p. 1801, 2015.

[11] T. Tigges, A. Pielmuş, M. Klum, A. Feldheiser, O. Hunsicker, and R. Orglmeister, "Model selection for the Pulse Decomposition Analysis of fingertip photoplethysmograms," in *Engineering in Medicine and Biology Society (EMBC), 2017 39th Annual International Conference of the IEEE*. IEEE, 2017, pp. 4014–4017.

[12] M. Sorelli, A. Perrella, and L. Bocchi, "Detecting vascular age using the analysis of peripheral pulse," *IEEE Transactions on Biomedical Engineering*, vol. 65, pp. 2742–2750, 2018.

[13] S. Zaunseder, A. Trumpp, H. Ernst, M. Förster, and H. Malberg, "Spatio-temporal analysis of blood perfusion by imaging photoplethysmography," in *Optical Diagnostics and Sensing XVIII: Toward Point-of-Care Diagnostics*, vol. 10501. International Society for Optics and Photonics, 2018, p. 105010X.

[14] F. Faul, E. Erdfelder, A.-G. Lang, and A. Buchner, "G* Power 3: A flexible statistical power analysis program for the social, behavioral, and biomedical sciences," *Behavior Research Methods*, vol. 39, no. 2, pp. 175–191, 2007.